ROS-mediated hypomethylation of *PRDX5* promotes *STAT3* binding and activates the *Nrf2* signaling pathway in NSCLC

XIANG CAO[1], XIN-MING CHEN[1], WEI-ZHANG XIAO[1], BEN LI[1], BO ZHANG[2], QIONG WU[2] and QUN XUE[1]

[1]Department of Thoracic Surgery, Affiliated Hospital of Nantong University; [2]Department of Clinical Medicine, Medical School of Nantong University, Nantong, Jiangsu 226001, P.R. China

Received December 12, 2019; Accepted November 16, 2020

DOI: 10.3892/ijmm.2020.4819

Abstract. Deoxyribonucleic acid (DNA) epigenetic modification has been linked to specific sequences of CpG islands and plays roles in the progression of lung cancer. In this study, it was found that peroxiredoxin-5 (*PRDX5*) was highly expressed in non-small cell lung cancer (NSCLC) tissues; however, its specific regulatory mechanisms and functions in NSCLC remain unknown. The present study therefore explored the regulatory mechanism of *PRDX5* under conditions of oxidative stress (OS) in NSCLC. The results revealed that 79 of 121 NSCLC patients exhibited demethylation in the *PRDX5* promoter region, which was related to the tumor, node and metastasis (TNM) stage (P=0.027). *PRDX5* messenger ribonucleic acid (mRNA) expression positively correlated with the demethylation status of the promoter region. The results of bisulfite sequencing polymerase chain reaction (BSP) revealed lower demethylation frequencies in H1299 cells treated with 0 μM H_2O_2, but maximum demethylation following treatment with 100 μM H_2O_2. Using chromatin immunoprecipitation (ChIP) and luciferase detection assays, the effective binding of *STAT3* to the transcriptional binding sites of the *PRDX5* promoter region was confirmed (2 sites confirmed: Site 1, -444 to -434 bp; and site 4, -1,417 to -1,407 bp). *STAT3* knockdown significantly decreased the protein expression of *PRDX5*, while the overexpression of *STAT3* significantly increased the protein levels of *PRDX5*. When *PRDX5* was overexpressed in lung cancer cells under conditions of OS, the levels of the epithelial-mesenchymal transition (EMT) biomarkers, E-cadherin and vimentin, were significantly decreased and increased, respectively. By contrast, *PRDX5* knockdown resulted in significantly increased E-cadherin and decreased vimentin protein expression levels. Ultimately, when *PRDX5*-small interfering RNA (siRNA) or pcDNA3.1-*PRDX5* expression vector were constructed and transfected into H1299 cells pre-treated with 100 μM H_2O_2, the nuclear factor (erythroid-derived 2)-like 2 (*Nrf2*) signaling pathway was inhibited or activated. All these results suggested that the reactive oxygen species (ROS)-mediated hypomethylation of *PRDX5* enhanced *STAT3* binding affinity with the promoter region, and resulted in the promotion of cell migration and invasion, as well as in the activation of the *Nrf2* signaling pathway in NSCLC. The demethylation status of the *PRDX5* promoter may thus be used as an epigenetic biomarker in NSCLC. *STAT3*/*PRDX5* signaling may also prove to be a potential strategy for the treatment of this type of cancer.

Correspondence to: Dr Qun Xue, Department of Thoracic Surgery, Affiliated Hospital of Nantong University, 20 Xisi Road, Nantong, Jiangsu 226001, P.R. China
E-mail: 13962800698@163.com

Key words: non-small cell lung carcinoma, DNA methylation, reactive oxygen species, *PRDX5*, epithelial-mesenchymal transition

Introduction

Currently, deaths from non-small cell lung cancer (NSCLC) account for 85% of lung cancer-related deaths worldwide (1). The disease is associated with a high degree of malignancy, and early and extensive metastasis, followed by a poor clinical prognosis (2). As lung cancers are the most lethal tumors in North America, their diagnosis and treatment are attracting increasing attention. Therefore, research on the molecular mechanisms of NSCLC is crucial for the investigation of the mechanisms responsible for the development of this tumor and for the identification of treatment strategies. In recent years, deoxyribonucleic acid (DNA) methylation, as one of the most common epigenetic modifications, has been linked to specific sequences of the CpG islands and plays an important role in the progression of lung cancer (3-6). Generally, DNA methylation results in the inactivation of gene expression (7,8), while demethylation in the promoter region activates gene transcription levels (9,10).

Reactive oxygen species (ROS), which are normally produced in and eliminated from all types of cells, exert physiological and pathological effects (11). In a tumor microenvironment (TME) of ischemia-hypoxia, ROS levels are commonly higher than in normal environments, which is crucial for the study of tumorigenesis and treatments (12,13). Peroxiredoxins (PRDXs) as a class of antioxidant enzymes that include 6 members, PRDX 1-6, which play a role in regulating cell proliferation, differentiation and apoptosis by modulating ROS (14). Recent studies have indicated that PRDXs participate in tumor progression, and upregulated levels of PRDXs have been suggested to be responsible for tumor prognosis

and drug resistance (15-17). In the present study, it was found that *PRDX5* was highly expressed in NSCLC tissues, while of note, there were obvious methyl islands in the promoter region. Therefore, it was hypothesized that the hypomethylation of the *PRDX5* gene promoter region may be related to the pathogenesis of NSCLC.

Signal transducers and activators of transcription (STATs) are a family of transcription factors (TFs) that can be activated by different cytokines and act as carriers during interaction between cytokines and receptors, maintaining the intracellular transmission of signals. Different STATs have their own specific functions; e.g., STAT4 and STAT1 induce T-helper 1 cell (T_h1) differentiation, whole STAT6 mediates T_h2 cell differentiation (18,19). *STAT3*, as the first-discovered member of the STAT family, was first defined as an acute response protein participating in various physiological or pathological processes; it is widely expressed in the human body and can be activated by a number of types of cytokines or by various stressors (20). Recent studies have demonstrated that the abnormal expression of *STAT3* is also found in a variety of tumors (21-23). However, the mechanisms through which *STAT3* promotes tumor progression remain unclear.

The present study aimed to explore the methylation status of the *PRDX5* gene promoter region in NSCLC. It was determined that the ROS-mediated hypomethylation of *PRDX5* promoted *STAT3* binding. Furthermore, the results revealed that the upregulation of *PRDX5* mediated by *STAT3* activated the nuclear factor (erythroid-derived 2)-like 2 (Nrf2) signaling pathway.

Materials and methods

Patients and tissue samples. NSCLC and adjacent non-cancerous tissues were obtained from 121 patients with NSCLC who underwent surgical resection at the Affiliated Hospital of Nantong University (Nantong, China) between January, 2006 and January, 2011. Detailed clinicopathological parameters of the patients are provided in Table I. The study protocol was approved by the Ethics Committee of Affiliated Hospital of Nantong University. Written informed consent was obtained from patients prior to collecting samples.

Cell lines and cell culture. The lung cancer cell lines, A549 (SCSP-503), H1299 (SCSP-589) and H157 (ATCC® CRL5802™), and the normal bronchial epithelial cell (EC) line, 16HBE (ATCC® PCS-300-040™), were purchased from the Shanghai Cell Bank of the Chinese Academy of Sciences or the American Type Culture Collection (ATCC). Following cell line authentication using short tandem repeat (STR) profiling, the cells were cultured in Dulbecco's modified Eagle's medium (DMEM; Gibco; Thermo Fisher Scientific, Inc.) supplemented with 10% fetal bovine serum (FBS, Gibco; Thermo Fisher Scientific, Inc.), 50 U/ml penicillin and 50 μg/ml streptomycin (Invitrogen; Thermo Fisher Scientific, Inc.); they were then incubated in a humidified atmosphere at 37˚C and 5% CO_2.

Establishment of model of oxidative stress (OS) induced by H_2O_2. H_2O_2 (Sigma-Aldrich; Merck KGaA) was used to the establishment of a model of OS. In brief, the lung cancer cell lines, A549, H1299 and H157, were pre-treated with various concentrations of H_2O_2 (0, 50, 100 or 200 μM) for 30 min of stimulation.

Methylation-specific and bisulfite sequencing polymerase chain reaction (MSP and BSP). The CpG island online prediction software (http://www.urogene.org/index.html) was used to predict the CpG islands of the *PRDX5* gene promoter. MSP was used to measure the methylation status of CpG islands in the *PRDX5* gene promoter region. The methylated (M) band indicated that CpG sites were methylated, while the unmethylated (U) band indicated unmethylated status. The patients with NSCLC were divided into the PRDX5-methylated and -unmethylated group (U/M ≥1, unmethylated; U/M <1, methylated). The demethylation ratio was calculated as U/(M + U). BSP was used to verify the methylation status of these islands. Extracted DNA samples isolated from NSCLC tissues and cells were modified with bisulfite reagents (Zymo Research) as per the manufacturer's instructions, which specified a change from unmethylated cytosine to thymine. The MSP primer pairs for *PRDX5* were as follows: PRDX5-MSP-M forward, 5'-GGGGTTGAATTT TATAGGGTAGATAC-3' and reverse, 5'-GACCTAACGAAA ATTTATACGACGA-3'; PRDX5-MSP-U forward, 5'-GGGGTT GAATTTTATAGGGTAGATAT-3' and reverse, 5'-AACCTA ACAAAAATTTATACAACAAC-3'. For BSP, bisulfite-treated DNA was amplified by PCR using the following primers: PRDX5-BSP forward, 5'-GGGTTGAATTTTATAGGGTAG ATA-3' and reverse, 5'-CTACTTACCCACAATCTACTAAAC TC-3'. PCR products were purified using the Wizard SV Gel and PCR Clean-up System and then cloned into a pGEM-T Easy Vector System (both from Promega Corporation). A total of 8 colonies were randomly selected for the extraction of plasmid DNA using a Promega Spin Mini kit (Promega Corporation) and the DNA was sequenced on an ABI 3130 Genetic Analyzer (Applied Biosystems; Thermo Fisher Scientific, Inc.).

Reverse transcription-quantitative PCR (qRT-PCR). RT-qPCR was used to determine *PRDX5* mRNA expression. Total RNA was extracted from tissues and cells using TRIzol reagent (Takara Bio, Inc.) as per manufacturer's instructions. First-strand complementary deoxyribonucleic acid (cDNA) was then synthesized using a PrimeScript RT Reagent kit and SYBR-Green I (Takara Bio, Inc.) was used for the qPCR analysis of the cDNA as per the manufacturer's instructions. The PCR thermocycling conditions were as follows: 95˚C for 5 min, (95˚C for 15 sec, 58˚C for 45 sec, and 72˚C for 60 sec) 40 cycles, and 72˚C for 1 min. Glyceraldehyde 3-phosphate dehydrogenase (*GAPDH*) was used as the internal control. The primer sequences for *PRDX5* and *GAPDH* were as follows: *PRDX5* forward, 5'-CCAATCAAGACACACCTG CC-3' and reverse, 5'-TCTTGAGACGTCGATTCCCA-3'; *GAPDH* forward, 5'-GAAGGTGAAGGTCGGAGTC-3' and reverse, 5'-GAAGATGGTGATGGGATTTC-3'. Quantities were calculated using the comparative $2^{-\Delta\Delta Cq}$ method (24). All steps were performed in triplicate.

Western blot analysis. Tissues and cells were lysed using radioimmunoprecipitation assay (RIPA) buffer containing protease inhibitors (Promega Corporation) to obtain total protein. The protein concentrations were then determined using a bicinchoninic acid (BCA) Protein Assay kit (Bio-Rad

Table I. Clinicopathological characteristics and *PRDX5* methylation in 121 patients with NSCLC.

Clinicopathological parameters	No. of patients	PRDX5 methylation		P-value
		Methylated (n=42)	Unmethylated (n=79)	
Age (years)				0.879
<60	53	18	35	
≥60	68	24	44	
Sex				0.830
Male	56	20	36	
Female	65	22	43	
Clinical TNM stage				
I-II	73	31	42	0.027[a]
III-IV	48	11	37	
Lymph node involvement				0.438
Negative	49	19	30	
Positive	72	23	49	
Differentiation				0.830
Well and moderate	65	22	43	
Poor	56	20	36	

[a]Indicates a statistically significant difference (P<0.05). PRDX5, peroxiredoxin-5; NSCLC, non-small cell lung cancer.

Laboratories, Inc.). Protein samples (containing 30 μg protein) were separated on 10% sodium dodecyl sulfate polyacrylamide gel electrophoresis (SDS-PAGE) gels and then transferred onto polyvinylidene difluoride (PVDF) membranes. The membranes were blocked with 5% skimmed milk for 1 h at room temperature and then incubated overnight with primary antibodies diluted to 1:1,000 at 4˚C. The following day, the membranes were further incubated with horseradish peroxidase (HRP)-conjugated secondary antibodies at room temperature for 1 h (1:2,000; cat no. 7056, Cell Signaling Technology, Inc.). GAPDH (1:1,000; cat no. A00227-1, Boster Biological Technology, Ltd.) was used as an internal reference. The immunoreactive proteins were detected using an enhanced chemiluminescence kit (Cell Signaling Technology, Inc.). The blots were then scanned on an Odyssey Fc Imaging System (Li-COR Biosciences) and the grayscale value was used for statistical analysis. The antibodies against *PRDX5* (1:1,000; cat no. ab180587), *STAT3* (1:1,000; cat no. ab76315), E-cadherin (1:1,000; cat no. ab40772), β-actin (1:1,000; cat no. ab8226), vimentin (1:1,000; cat no. ab92547), *Nrf2* (1:1,000; cat no. ab89443) and reduced nicotinamide adenine dinucleotide phosphate (NADPH) dehydrogenase [quinone] 1 (*NQO1)* (1:1,000; cat no. ab80588) were all from Abcam.

Construction and transfection of plasmids and small interfering RNA (siRNA). The overexpression plasmids (pcDNA3.1-*STAT3* and *PRDX5)* and the control (pcDNA3.1-vector), siRNAs against *STAT3* and *PRDX5* [si-*STAT3* (CGTCATTAGCAG AATCTCATT) and si-*PRDX5* (GGAATCGACGTCTCA AGAGGT), respectively] and corresponding negative-control (NC) siRNAs (si-NC, GCAGATAGGTAGGCGTTAT) were all designed and synthesized by Guangzhou RiboBio Co., Ltd. The process of transient cell transfection was conducted using standard methods as per manufacturer's instructions. Briefly, cells were maintained in medium with fetal bovine serum (FBS, 10%) until the confluence reached 70-80%, and all the oligonucleotides (RNA and DNA) were then transfected into the cells using Lipofectamine 2000 (Invitrogen; Thermo Fisher Scientific, Inc.). following 48 h of transfection, the transfection efficiency was detected by western blot analysis.

Chromatin immunoprecipitation (ChIP) assay. In order to explore the transcription factors that may be involved in the regulation of *PRDX5* gene expression, the online software Jaspar (http://jaspar.genereg.net) was used to predict the transcription factors that may bind to the promoter region. ChIP assay was then performed using a ChIP kit (magnetic beads; Cell Signaling Technology, Inc.) as per the manufacturer's instructions. Briefly, DNA-protein complexes were cross-linked with 1% formaldehyde, and 1% SDS Lysis Buffer was then added followed by sonication. The used antibody to immunoprecipitated anti-*STAT3* (1:20, ab76315; Abcam) or normal mouse immunoglobulin G (IgG, 1:200, cat. no. 554002, BD Biosciences) was added at 4˚C for 12 h. DNA was then purified out of the antibody-protein-DNA complex and used for PCR. Specific ChIP primers for detailed sequences of the *PRDX5* promoter were as follows: Site 1 forward, TATTGGATAGCC AGGAGAACC and reverse, GGAACCTCCTGCTGAGAC G (131 bp); site 2 forward, ATGTCGCCGCACAAACT and reverse, CCCACAAACACGAGAAGTTCC (147 bp); site 3 forward, GAAACCGCTTTTGGTTTTAAAC and reverse, CCAACCCTTGACCCAATGAC (94 bp); site 4 forward, CTC AGGGGGTAGGAGAGCA and reverse, GGTTTAAAACCA AAAGCGGT (182 bp); and site 5 forward, CTCTCCTCC CCCTCCTAGGG and reverse, TGGCCTCCATCCCCTTCC (188 bp). The following PCR conditions were used: 95˚C for

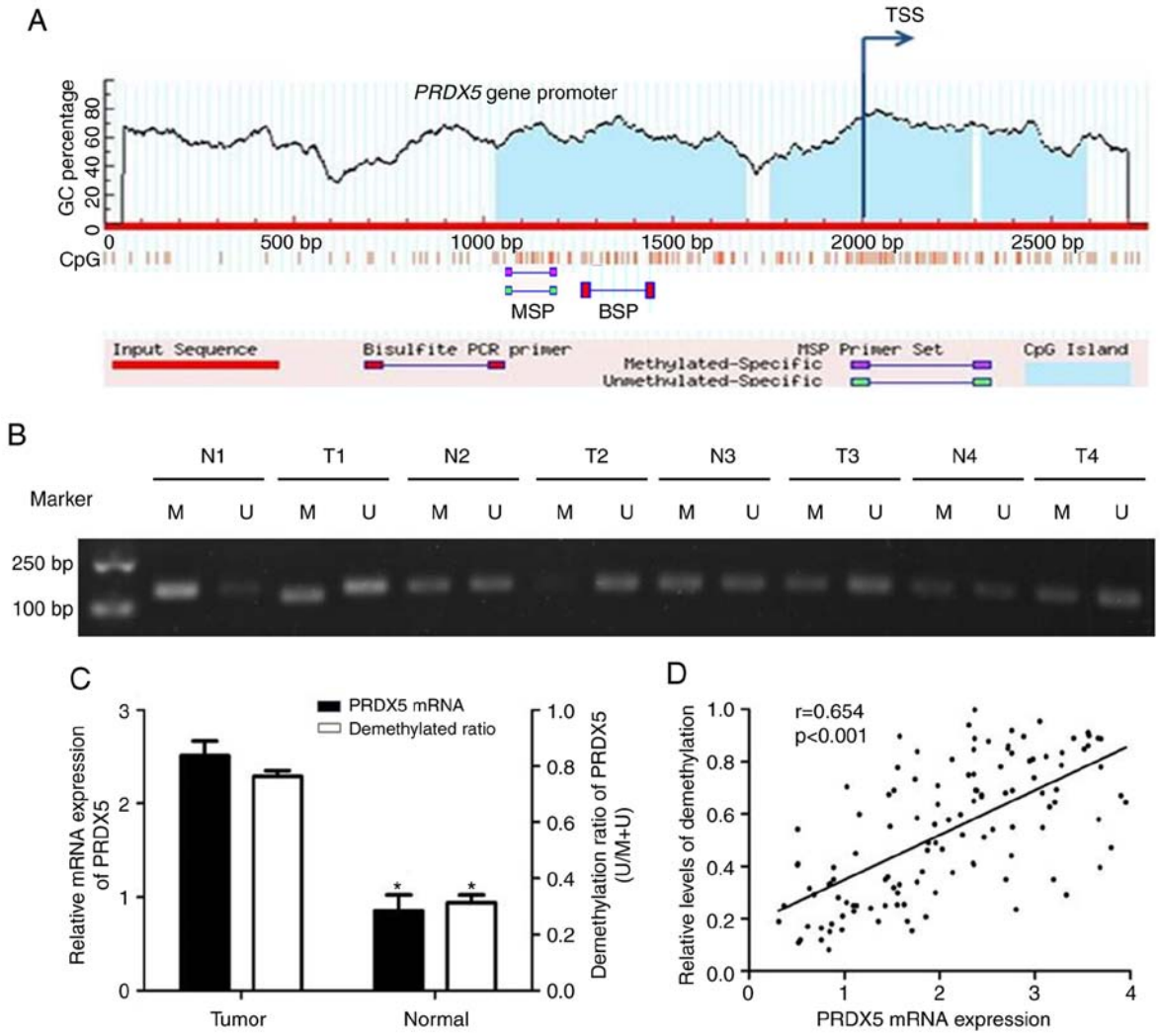

Figure 1. Demethylation status of the CpG islands in the *PRDX5* gene promoter in NSCLC. (A) Online prediction of CpG islands around the *PRDX5* gene promoter region. The light blue areas represent the potential CpG islands. (B) Representative methylation analysis results by MSP in NSCLC tissues and adjacent normal lung tissues. M, methylation; U, unmethylation. (C) Relative expression of *PRDX5* mRNA significantly increased in tumor tissues than that in normal ones and demethylation ratio of *PRDX5* gene promoter showed significantly higher in tumor tissues than that in the adjacent normal ones. *P<0.05, vs. *PRDX5* mRNA or demethylated ratio in the respective tumor or normal group. (D) Correlation analysis between the demethylation ratio by MSP and PRDX5 mRNA expression by qPCR. *PRDX5*, peroxiredoxin-5; NSCLC, non-small cell lung cancer; MSP, Methylation-specific PCR.

5 min, 95˚C for 30 sec, 55-60˚C for 30 sec, and 72˚C for 30 sec for a total of 30 cycles, and then 72˚C for 10 min. The acquired products were observed using agarose gel electrophoresis.

Luciferase reporter assay (LRA). The sequences (760 and 640) from upstream to the start of the *PRDX5* gene were cloned into pGL3 luciferase reporter vector (Promega Corporation), and were transfected into the cells with Lipofectamine 2000 (Invitrogen; Thermo Fisher Scientific, Inc.) together with internal reference vectors, phRL-TK. Luciferase activities were detected using a Dual Luciferase Assay System (Promega Corporation) at 48 h following transfection in triplicate, and *Renilla* luciferase activity served as the internal control.

DNA methylation in vitro. PGL3-640 and PGL3-760 were treated with DNA *Sss*I methylase (New England Biolabs) for 4 h at 37˚C; and these plasmids were incubated similarly but without *Sss*I methylase (unmethylated control). The plasmids were then further purified with a PCR product clean-up kit (Axygen). The unmethylated or methylated activities of PGL3-640 and PGL3-760 were measured as per the above methods.

Cell migration and invasion assay. Cell migration and invasion were detected using Transwell chambers (Corning, Inc.) coated with or without Matrigel (no. 356234; BD Biosciences). A total of $2x10^4$ cells in 100 μl were added to the chambers with serum-free DMEM, while the lower chambers were filled with culture medium containing 10% FBS in a humidified 5% CO_2 atmosphere at 37˚C. After 48 h, the invading or migrating cells were fixed with 4% paraformaldehyde and stained with 0.5% crystal violet (Sigma-Aldrich; Merck KGaA) for 20 min at room temperature. Cells were counted under a microscope (Leica DM2500, Leica Microsystems, Inc.) at x200 magnification.

Statistical analysis. SPSS software version 17.0 (IBM Corp.) was used for statistical analysis. All data are expressed as the

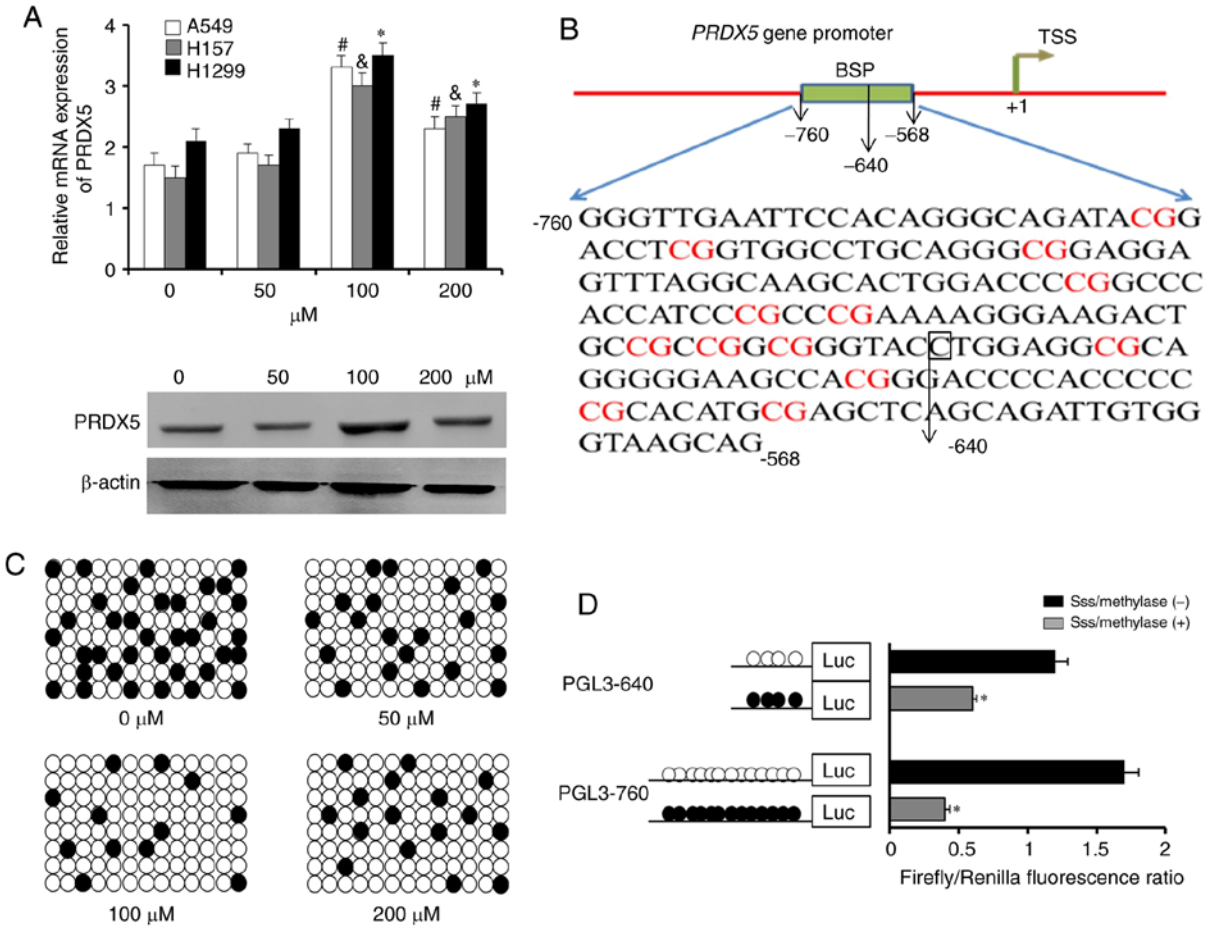

Figure 2. Hypomethylation of specific CpG sites within the *PRDX5* promoter promotes transcriptional activities under oxidative stress. (A) Relative *PRDX5* mRNA levels (upper panel) in different cell lines and protein expression in H1299 cells (lower panel) that were pre-treated with various concentrations of H_2O_2 (0, 50, 100 and 200 μM). $^{*,\#,\&}$P<0.05, vs. the respective cell line in the untreated groups. (B) Schematic BSP regions (from -760 to -568 bp) showing locations of the 13 CpG sites in the *PRDX5* gene promoter region. (C) Bisulfite sequencing analysis of the demethylation status of the *PRDX5* gene promoter under different conditions of oxidative stress. Each oval indicates clones from different cell lines. Vertical row represents the number of clones sent for bisulfite sequencing and horizontal row represents CpG numbers. Black circles represent the methylated clones and white circles indicate an unmethylated status. (D) Treatment with S*ssI* methylase in 2 luciferase constructs *in vitro*. *P<0.05, vs. S*ssI* methylase (-) group. Independent data results were repeated 3 times. *PRDX5*, peroxiredoxin-5; BSP, bisulfite sequencing PCR.

means ± standard deviation (SD) in triplicate. A paired or independent sample t-test was used to analyze differences between 2 groups. For the comparison of multiple groups, differences were analyzed by one-way analysis of variance (ANOVA). When ANOVA detected significant differences, the data of the variables of each experimental group were compared with that of the control group using a Dunnett's post hoc test. An χ^2 test was used to examine the association between the promoter methylation of *PRDX5* and the patient clinicopathological parameters. Correlation analysis was performed using Spearman's correlation coefficient (SCC). A value of P<0.05 was considered to indicate a statistically significant difference.

Results

PRDX5 upregulation in NSCLC tissues is associated with CpG island demethylation in the promoter region. First, to determine whether *PRDX5* upregulation in NSCLC tissues was associated with the demethylation of CpG islands in the promoter region, the CpG island online prediction software (http://www.urogene.org/index.html) was searched and it was found that 3 CpG islands existed near the transcription start site (Fig. 1A). Since the promoter region upstream of TSS may have more transcription factors binding to start gene transcription, and the length of the first CpG island is longer, the 1st one was selected to design primers. Subsequently, 121 pairs of NSCLC tissues and adjacent non-cancerous tissues were analyzed to determine the methylation status of CpG islands in the *PRDX5* promoter region by MSP. The results revealed that 79 of the 121 patients with NSCLC exhibited *PRDX5* promoter demethylation, and that the demethylation was associated with tumor, node and metastasis (TNM) stage (P=0.027), but not with age, sex, lymph nodes or differentiation (Table I). A total of 8 representative cases of MSP results are presented in Fig. 1B. All the 121 tumor tissues exhibited a significantly higher demethylation ratio in the *PRDX5* promoter region compared with that in adjacent non-cancerous tissues (P<0.05; Fig. 1C). Additionally, the results of RT-qPCR revealed that *PRDX5* mRNA expression was upregulated in NSCLC tissues compared with adjacent tissues (P<0.05, Fig. 1C). As shown in Fig. 1D, *PRDX5* mRNA expression positively correlated with the demethylation status of the promoter region.

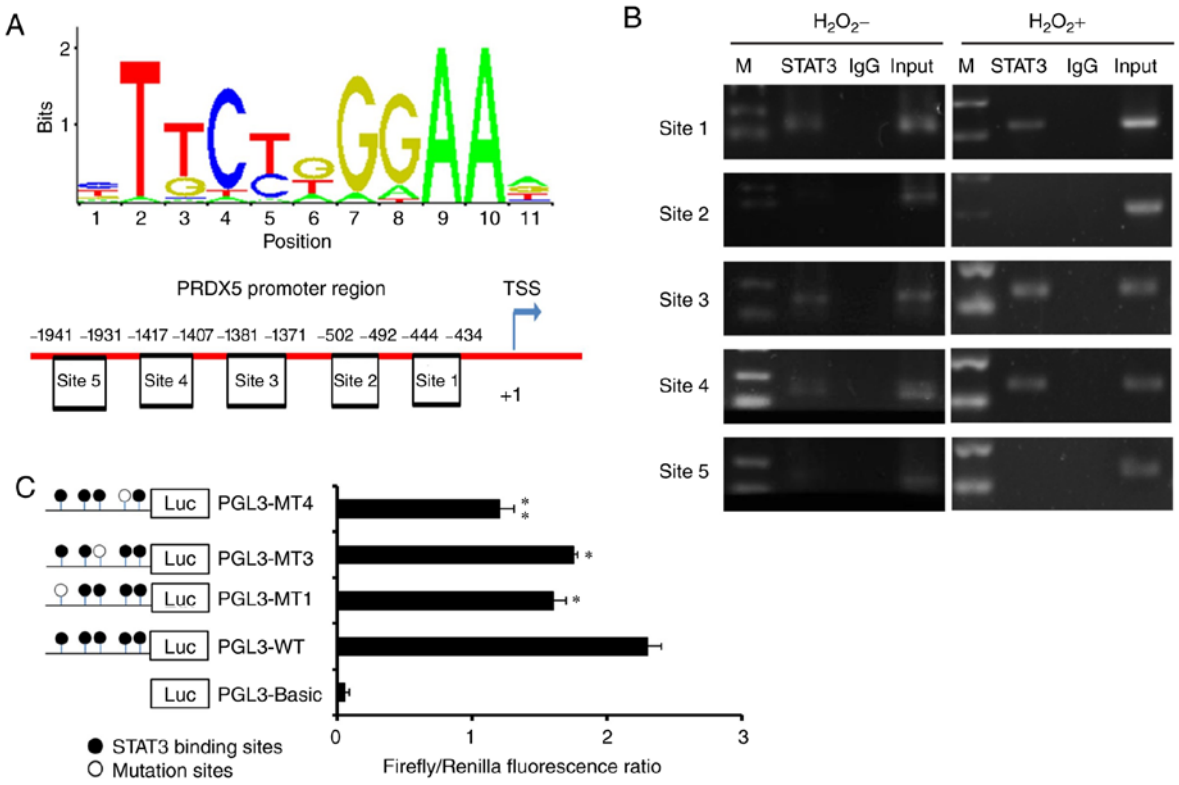

Figure 3. Promoted binding of *STAT3* to the *PRDX5* gene promoter region due to DNA demethylation. (A) The predicted potentially binding sequence and binding position of *STAT3* binding to the transcription factor binding site near the promoter region of *PRDX5*. TSS, transcription start site. (B) ChIP assay showing the direct binding of *STAT3* to the *PRDX5* gene promoter in H1299 cells. The ChIP-enriched DNA fragments of the *PRDX5* gene promoter using IgG and an anti-*STAT3* antibody were amplified by PCR. Total input was used as a positive control. (C) Sequential mutation analysis identified the direct *STAT3* binding sites in the *PRDX5* gene promoter region by determination of relative luciferase activities. Data are presented as the means ± SD. *P<0.05, **P<0.01, vs. the PGL3-WT group. *PRDX5*, peroxiredoxin-5; *STAT3*, signal transducer and activator of transcription 3.

Hypomethylation of specific CpG sites within the PRDX5 promoter region promotes transcriptional activities under conditions of OS. To obtain further details of the demethylation status of specific CpG sites within the *PRDX5* promoter region under conditions of OS, an *in vitro* model of ROS was induced using H_2O_2 (Sigma-Aldrich; Merck KGaA). A 193 bp length of PCR products (-760 to -568 bp) was analyzed following sodium bisulfite treatment as part of the BSP method. The lung cancer cell lines, A549, H1299 and H157, were pre-treated with various concentrations of H_2O_2 (0, 50, 100 or 200 μM). Following 30 min of stimulation, the results of RT-qPCR for relative *PRDX5* mRNA expression revealed the significant upregulation of *PRDX5* expression in the 100 μM H_2O_2 group in the 3 cell lines (Fig. 2A, upper panel); similar results were obtained for protein expression in the H1299 cells (Fig. 2A, bottom panel). The H1299 cells that had been treated with 100 μM H_2O_2 were then selected for BSP. As shown in Fig. 2B, the sequencing region contained 13 CpG sites from -760 to -568 bp. The results of BSP revealed lower demethylation frequencies in H1299 cells treated with 0 μM H_2O_2, but maximum demethylation in those treated with 100 μM H_2O_2 (Fig. 2C).

Finally, to determine which CpG sites were responsible for the demethylation-related activation of the *PRDX5* gene under conditions of OS, two *PRDX5* gene promoter regions (PGL3-640 and PGL3-760) were constructed; these were then treated with *SssI* methylase *in vitro* and transfected into H1299 cells that had been pre-treated with 100 μM H_2O_2 (Fig. 2D). Compared with the treated promoter constructs, the untreated constructs exhibited a significantly greater demethylation and promoter activity. No marked differences in the promoter activity of PGL3-640 or PGL3-760 were observed between the *SssI* methylase-treated and untreated groups. These results indicated that the region of the CpG sites from -640 to -568 bp may play as an important role in regulating *PRDX5* gene transcription.

Promoted binding of STAT3 to the PRDX5 gene promoter region due to DNA demethylation. To explore related TFs that may be involved in the regulation of *PRDX5* expression, the TFs that could potentially bind to the TF binding site near the promoter region were predicted using the website, http://jaspar.genereg.net/ (Fig. 3A). A total of 5 potential *STAT3* binding sites were screened near the *PRDX5* promoter region (site 1, -444 to -434; site 2, -502 to -492; site 3, -1,381 to -1,371; site 4, -1,417 to -1,407; site 5, -1,941 to -1,931 bp). Subsequently, the actual binding of *STAT3* to the transcriptional binding sites of the DNA promoter region under conditions of OS was examined by ChIP assay. The results revealed that *STAT3* could obviously bind to sites 1, 3 and 4, but not to sites 2 or 5 (Fig. 3B and C).

Finally, to further verify the effective binding sites indicated by the results of ChIP assay, mutant plasmids that were directed against each of sites 1, 3 and 4 were constructed. The results of luciferase detection revealed a significant decrease in the PGL3-MT1 and PGL3-MT4 regions (Fig. 3C). This indicated that sites 1 and 4 were the effective TF binding sites for *PRDX5* gene transcription.

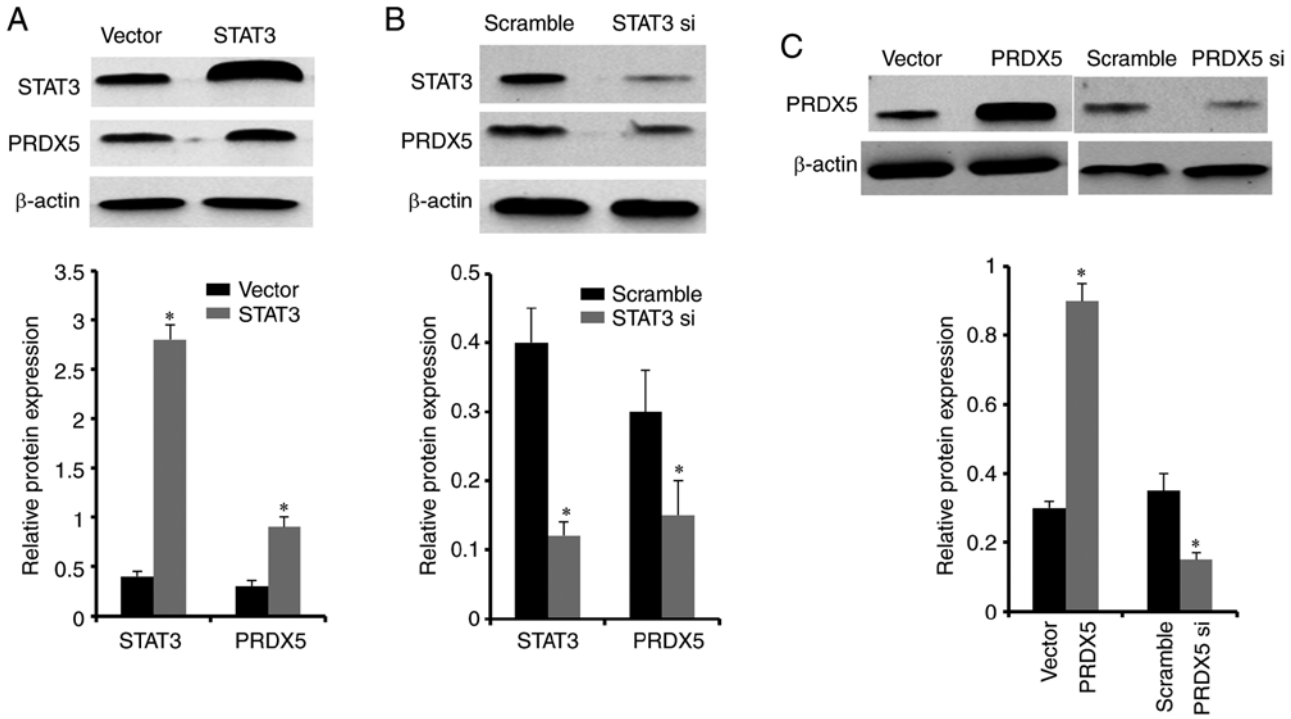

Figure 4. *STAT3* mediates the regulation of *PRDX5* expression. (A) *STAT3* protein expression significantly increased in the cells when transfected with pcDNA3.1-*STAT3* and significantly upregulated the *PRDX5* protein expression level (*P<0.05, vs. control vector group). Data are presented as the means ± SD. (B) *STAT3* protein expression significantly decreased in the cells when transfected with STAT3 siRNA compared with that of cells transfected with the scramble and significantly downregulated the *PRDX5* protein expression level (*P<0.05, vs. scramble group). Data are presented as the means ± SD. (C) *PRDX5* protein expression levels significantly increased or decreased when transfected with pcDNA3.1-*PRDX5* or siRNA, respectively (*P<0.05, vs. control vector or scramble group). *PRDX5*, peroxiredoxin-5; *STAT3*, signal transducer and activator of transcription 3.

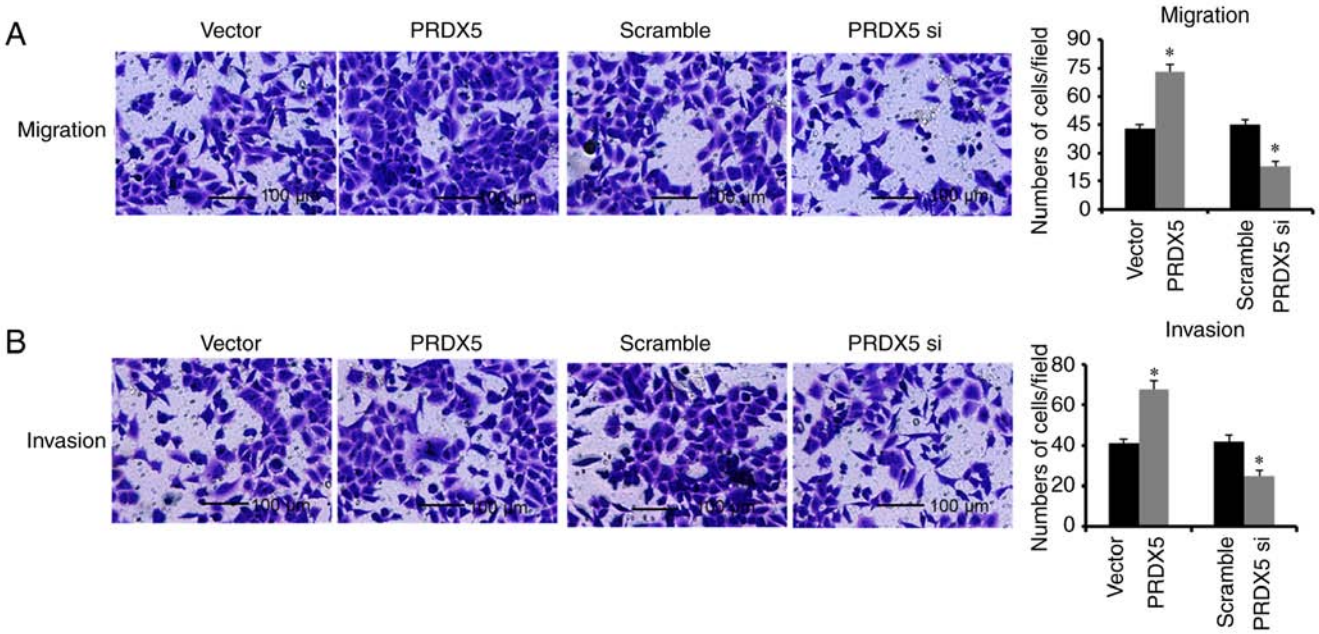

Figure 5. Effects of *PRDX5* on cell migration and invasion. (A) Upregulation of *PRDX5* significantly promoted cell migration, while the downregulation of *PRDX5* yielded opposite results (*P<0.05, vs. control vector or scramble group). Data are presented as the means ± SD. (B) Upregulation of *PRDX5* significantly promoted cell invasion, while downregulation of *PRDX5* yielded opposite results (*P<0.05, vs. control vector or scramble group). Magnification, x200. Data are presented as the means ± SD. *PRDX5*, peroxiredoxin-5.

STAT3-regulated PRDX5 signaling affects the migration and invasion of lung cancer cells under conditions of OS. To further demonstrate that *STAT3* was involved in regulating *PRDX5* expression, *STAT3* siRNA and the expression plasmid, pcDNA3.1-*STAT3* were constructed. These were then transfected each into H1299 cells pre-treated with 100 μM H_2O_2. After 48 h, the results of western blot analysis revealed that *STAT3* protein expression was significantly

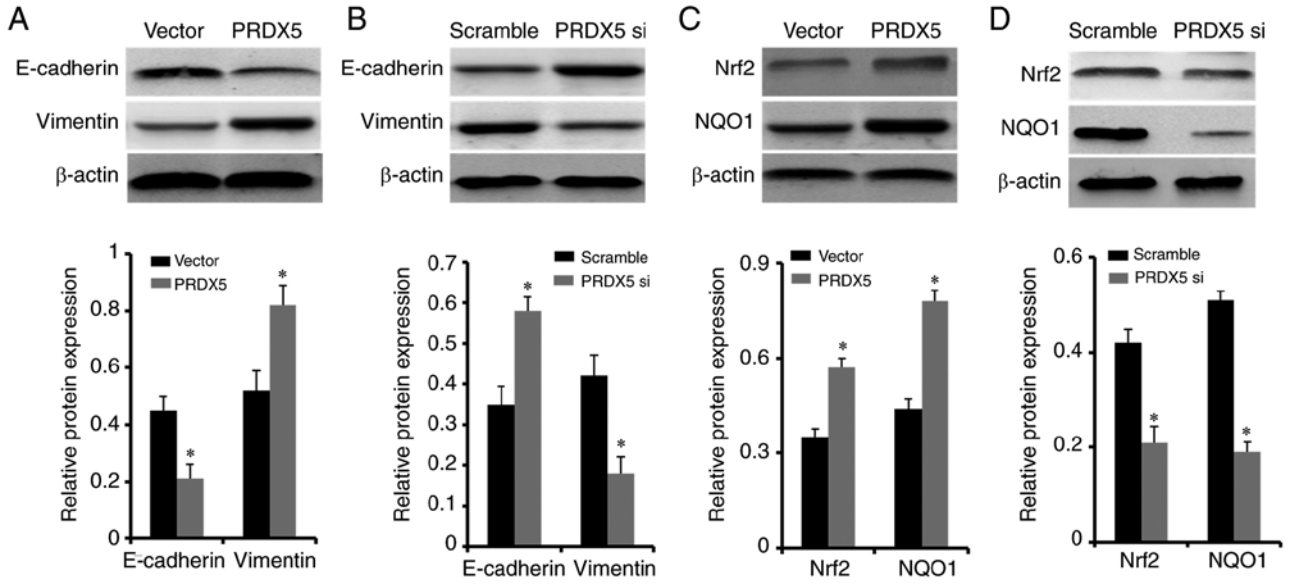

Figure 6. *PRDX5* affects EMT phenotypes and the oxidative stress signaling pathway. (A) Overexpression of *PRDX5* significantly downregulated E-cadherin expression, while it upregulated the vimentin protein expression level (*P<0.05, vs. control vector group). Data are presented as the means ± SD. (B) Knockdown of *PRDX5* completely reversed the above-mentioned results (*P<0.05, vs. scramble group). Data are presented as the means ± SD. (C) Overexpression of *PRDX5* significantly increased the protein expression level of Nrf2 and NQO1 (*P<0.05, vs. control vector group). Data are presented as means ± SD. (D) Knockdown of *PRDX5* significantly downregulated the expression of Nrf2 and NQO1 protein (*P<0.05, vs. scramble group). Data are presented as the means ± SD. *PRDX5*, peroxiredoxin-5; Nrf2, nuclear factor (erythroid-derived 2)-like 2; NQO1, nicotinamide adenine dinucleotide phosphate (NADPH) dehydrogenase [quinone] 1.

decreased in the *STAT3* siRNA group compared with the scramble group, while protein expression levels were significantly increased in the group transfected with pcDNA3.1-*STAT3* compared with the control vector group. In addition, *STAT3* knockdown significantly decreased the protein expression of *PRDX5*, while the overexpression of *STAT3* significantly increased the protein level of *PRDX5* (Fig. 4A and B).

To further clarify the effects of *PRDX5* on the migration and invasion of lung cancer cells under conditions of OS, *PRDX5* siRNA and the corresponding overexpression plasmid pcDNA3.1-*PRDX5* were constructed and transfected into H1299 cells pre-treated with 100 μM H_2O_2. The results indicated that the PRDX5 protein levels significantly decreased following transfection with *PRDX5* siRNA (Fig. 4C). In addition, the cell migratory and invasive abilities were also significantly suppressed following the knockdown of *PRDX5* (Fig. 5). By contrast, PRDX5 protein expression significantly increased following transfection with pcDNA3.1-*PRDX5* (Fig. 4C), and the cell migratory and invasive abilities were also increased (Fig. 5). At the same time, when *PRDX5* was overexpressed in lung cancer cells under conditions of OS, the levels of the epithelial-mesenchymal transition (EMT) biomarkers, E-cadherin and vimentin, were significantly decreased and increased, respectively (Fig. 6A). Conversely, *PRDX5* knockdown resulted in significantly increased E-cadherin and decreased vimentin protein expression levels (Fig. 6B). The above-mentioned results indicated that *PRDX5* may be regulated by *STAT3*, and that it affected the migratory and invasive abilities of lung cancer cells under conditions of OS, promoting the EMT phenotype.

PRDX5 activates the Nrf2 signaling pathway in lung cancer cells under conditions of OS. To verify that *PRDX5* can activate Nrf2 signaling under conditions of OS, *PRDX5* siRNA and pcDNA3.1-*PRDX5* were transfected into H1299 cells pre-treated with 100 μM H_2O_2. The expression of key molecules of OS, Nrf2 and NQO1, was significantly upregulated when the cells were transfected with pcDNA3.1-*PRDX5* (Fig. 6C). By contrast, *PRDX5* knockdown resulted in significantly decreased protein expression levels of *Nrf2* and *NQO1* (Fig. 6D). These results indicated that *PRDX5* may be involved in the activation of the *Nrf2* signaling pathway in lung cancer cells under conditions of OS.

Discussion

Lung cancer is currently a malignancy with an unclear molecular mechanism, particularly as regards NSCLC (25). As NSCLC progresses, ROS levels are increased in cancer cells compared with in normal cells, mainly due to the abnormal metabolic level in tumors; this leads to the overproduction of ROS in ischemic hypoxic environments. As a peroxiredoxin family member, *PRDX5* plays an important role in maintaining intracellular ROS or peroxide levels induced by cytokines (26). In the present study, H1299 cells were pre-treated with 100 μM H_2O_2 to establish the ROS model *in vitro*. Although this induced ROS and the upregulated endogenous expression of *PRDX5*, this does not have an impact on the results of subsequent experiments, as it is the result of the comparison between the two groups. As the results were based on the comparison between the 2 groups, and are from an epigenetic perspective, it was clarified that the upregulated expression of the *PRDX5* gene mainly participated in the migration and invasion of lung cancer cells under conditions of OS and activated the *Nrf2* signaling pathway.

DNA methylation is one of the most common means of epigenetic regulation. For example, it plays an important role in

the modulation of cancers and inflammation or tissue-damaging pain (27-29). In the present study, it was found that *PRDX5* was upregulated due to the demethylation of its promoter region, and at the same time, that different OS levels led to varying degrees of demethylation and *PRDX5* mRNA expression. This demonstrated that OS promoted *PRDX5* expression by demethylating the promoter region. There were 2 possibilities: The one is that the number of samples was still not sufficient to explain the problem. The other is that it was really no association between the two.

Using ChIP assay, it was verified that *STAT3* functioned as a TF in binding to the *PRDX5* gene promoter region. In addition, to the best of our knowledge, the present study also demonstrated for the first time that the ability of *STAT3* to bind to this region was markedly enhanced in NSCLC under conditions of OS. This enhanced affinity promoted *PRDX5* expression, while the mutation of the binding site between the *PRDX5* gene promoter region and *STAT3* resulted in a significantly decreased *PRDX5* expression. From an epigenetic perspective, these results may have been caused by the hypomethylation of the *PRDX5* gene promoter region, leading to enhanced affinity between binding sites. Choi *et al* (30) reported that the overexpression of *PRDX5* suppressed the TGF-β induced upregulation of *STAT3* phosphorylation. Perhaps under certain specific conditions (tumor or non-tumor conditions), *PRDX5* and *STAT*3 may have a negative feedback regulation, forming a negative feedback regulation loop to perform specific functions. The present study did not notice this point; thus, the authors aim to continue to explore the association between the 2 genes in the future. In addition, it is hypothesized that the mutation of all 3 binding sites will not disrupt *STAT3* binding completely, for the binding sites are only acquired by prediction and identification by experiments; it can also not be ruled out that there may be other binding sites.

EMT is an important biological process in the migration and invasion of malignant tumor cells derived from ECs (31). It plays an important role in embryonic development (32), chronic inflammation (33), cancer metastasis (34) and a variety of fibrotic diseases (35), the main characteristic of which is a decrease in the expression of cell adhesion molecules (CAMs), such as E-cadherin. The cytoskeleton of cytokeratin is transformed into vimentin, which has the morphological characteristics of mesenchymal cells. Ahn *et al* reported that *PRDX5* promoted EMT in colon cancer (36). In contrast to this aforementioned study, the present study found that the hypomethylation of *PRDX5* promoted *STAT3* binding, and promoted cell migration, invasion and EMT progression, which manifested as E-cadherin downregulation and vimentin upregulation. By contrast, the lower expression of *PRDX5* suppressed cell migration, invasion and EMT. These results indicated that *PRDX5* may affect cell migration and invasion by activating EMT.

The *Nrf2* antioxidant-responsive element (ARE) pathway is one of the most important endogenic anti-OS pathways to be discovered to date. There is evidence to indicate that when activated, this pathway can inhibit the degradation of *Nrf2* protein mediated by ubiquitin, stabilize the concentration of *Nrf2* protein in cytoplasm, and enhance the transcriptional activity of *Nrf2* protein (37,38). The results of the present study revealed that *PRDX5* overexpression under conditions of OS significantly increased the protein levels of *Nrf2* and *NQO1*, which are key proteins of the *Nrf2*/ARE signaling pathway. These results may provide a strategy for the treatment of NSCLC.

In conclusion, the present study demonstrated that the ROS-mediated hypomethylation of *PRDX5* enhanced *STAT3* binding affinity with the *PRDX5* gene promoter region, and promoted cell migration and invasion, as well as the activation of the *Nrf2* signaling pathway in NSCLC. The demethylation status of the *PRDX5* promoter may be used as an NSCLC epigenetic biomarker and *STAT3*/*PRDX5* signaling may prove to be a potential target in the treatment of NSCLC.

Acknowledgements

Not applicable.

Funding

This study was supported by the National Natural Science Foundation of China (grant no. 8157101409) and the Nantong Science and Technology Project (grant no. MS12017010-2).

Availability of data and materials

All data generated or analyzed during the current study are included in this published article.

Authors' contributions

XC and QX designed the study. XC, XMC and WZX performed the experiments. XMC and BL collected the data and performed the analysis. BZ and QW collected the data. XC and QX wrote the article. All authors read and approved the manuscript.

Ethics approval and consent to participate

The study protocol was approved by the Ethics Committee of Affiliated Hospital of Nantong University. Written informed consent was obtained from all patients prior to sample collection.

Patient consent for publication

Not applicable.

Competing interests

The authors declare that they have no competing interests.

References

1. Siegel RL, Miller KD and Jemal A: Cancer statistics, 2017. CA Cancer J Clin 67: 7-30, 2017.
2. Liu SV and Giaccone G: Lung cancer in 2013: Refining standard practice and admitting uncertainty. Nat Rev Clin Oncol 11: 69-70, 2014.
3. Song X, Zhao C, Jiang L, Lin S, Bi J, Wei Q, Yu L, Zhao L and Wei M: High PITX1 expression in lung adenocarcinoma patients is associated with DNA methylation and poor prognosis. Pathol Res Pract 214: 2046-2053, 2018.

4. Zhang X, Rong X, Chen Y and Su L: Methylation-mediated loss of SFRP2 enhances invasiveness of non-small cell lung cancer cells. Hum Exp Toxicol 37: 155-162, 2018.
5. Chen L, Wang Y, Liu F, Xu L, Peng F, Zhao N, Fu B, Zhu Z, Shi Y, Liu J, *et al*: A systematic review and meta-analysis: Association between MGMT hypermethylation and the clinicopathological characteristics of non-small-cell lung carcinoma. Sci Rep 8: 1439, 2018.
6. Raungrut P, Petjaroen P, Geater SL, Keeratichananont W, Phukaoloun M, Suwiwat S and Thongsuksai P: Methylation of 14-3-3s gene and prognostic significance of 14-3-3s expression in non-small cell lung cancer. Oncol Lett 14: 5257-5264, 2017.
7. Zhou Y, Qiu XP, Li ZH, Zhang S, Rong Y, Yang GH and Fang-Zheng: Clinical significance of aberrant cyclin-dependent kinase-like 2 methylation in hepatocellular carcinoma. Gene 683: 35-40, 2019.
8. Peters I, Dubrowinskaja N, Hennenlotter J, Antonopoulos WI, Von Klot CAJ, Tezval H, Stenzl A, Kuczyk MA and Serth J: DNA methylation of neural EGFL like 1 (NELL1) is associated with advanced disease and the metastatic state of renal cell cancer patients. Oncol Rep 40: 3861-3868, 2018.
9. Li F, Xue ZY, Yuan Y, Huang SS, Fan YH, Zhu X and Wei L: Upregulation of CXCR4 through promoter demethylation contributes to inflammatory hyperalgesia in rats. CNS Neurosci Ther 24: 947-956, 2018.
10. Jiang C, Guo J, Cheng H and Feng YH: Induced expression of endogenous CXCR4 in iPSCs by targeted CpG demethylation enhances cell migration toward the ligand CXCL12. Inflammation 42: 20-34, 2019.
11. Kang D and Hamasaki N: Mitochondrial oxidative stress and mitochondrial DNA. Clin Chem Lab Med 41: 1281-1288, 2003.
12. Nogueira V and Hay N: Molecular pathways: Reactive oxygen species homeostasis in cancer cells and implications for cancer therapy. Clin Cancer Res 19: 4309-4314, 2013.
13. Lin S, Li Y, Zamyatnin AA Jr, Werner J and Bazhin AV: Reactive oxygen species and colorectal cancer. J Cell Physiol 233: 5119-5132, 2018.
14. Knoops B, Goemaere J, Van der Eecken V and Declercq JP: Peroxiredoxin 5: Structure, mechanism, and function of the mammalian atypical 2-Cys peroxiredoxin. Antioxid Redox Signal 15: 817-829, 2011.
15. Kim B, Park J, Chang KT and Lee DS: Peroxiredoxin 5 prevents amyloid-beta oligomer-induced neuronal cell death by inhibiting ERK-Drp1-mediated mitochondrial fragmentation. Free Radic Biol Med 90: 184-194, 2016.
16. Kim B, Kim YS, Ahn HM, Lee HJ, Jung MK, Jeong HY, Choi DK, Lee JH, Lee SR, Kim JM and Lee DS: Peroxiredoxin 5 overexpression enhances tumorigenicity and correlates with poor prognosis in gastric cancer. Int J Oncol 51: 298-306, 2017.
17. Byun JM, Kim SS, Kim KT, Kang MS, Jeong DH, Lee DS, Jung EJ, Kim YN, Han J, Song IS, *et al*: Overexpression of peroxiredoxin-3 and -5 is a potential biomarker for prognosis in endometrial cancer. Oncol Lett 15: 5111-5118, 2018.
18. Baumann C, Bonilla WV, Fröhlich A, Helmstetter C, Peine M, Hegazy AN, Pinschewer DD and Löhning M: T-bet- and STAT4-dependent IL-33 receptor expression directly promotes antiviral Th1 cell responses. Proc Natl Acad Sci USA 112: 4056-4061, 2015.
19. Koch MA, Thomas KR, Perdue NR, Smigiel KS, Srivastava S and Campbell DJ: T-bet(+) Treg cells undergo abortive Th1 cell differentiation due to impaired expression of IL-12 receptor β2. Immunity 37: 501-510, 2012.
20. Akira S, Nishio Y, Inoue M, Wang XJ, Wei S, Matsusaka T, Yoshida K, Sudo T, Naruto M and Kishimoto T: Molecular cloning of APRF, a novel IFN-stimulated gene factor 3 p91-related transcription factor involved in the gp130-mediated signaling pathway. Cell 77: 63-71, 1994.
21. Jiang LH, Hao YL and Zhu JW: Expression and prognostic value of HER-2/neu, STAT3 and SOCS3 in hepatocellular carcinoma. Clin Res Hepatol Gastroenterol 43: 282-291, 2019.
22. Fathi N, Rashidi G, Khodadadi A, Shahi S and Sharifi S: STAT3 and apoptosis challenges in cancer. Int J Biol Macromol 117: 993-1001, 2018.
23. Chu Y, Wang Y, Peng W, Xu L, Liu M, Li J, Hu X, Li Y, Zuo J and Ye Y: STAT3 activation by IL-6 from adipose-derived stem cells promotes endometrial carcinoma proliferation and metastasis. Biochem Biophys Res Commun 500: 626-631, 2018.
24. Livak KJ and Schmittgen TD: Analysis of relative gene expression data using real-time quantitative PCR and the 2(-Delta Delta C(T)) method. Methods 25: 402-408, 2001.
25. Raju S, Joseph R and Sehgal S: Review of checkpoint immunotherapy for the management of non-small cell lung cancer. Immunotargets Ther 7: 63-75, 2018.
26. Sabharwal SS, Waypa GB, Marks JD and Schumacker PT: Peroxiredoxin-5 targeted to the mitochondrial intermembrane space attenuates hypoxia-induced reactive oxygen species signalling. Biochem J 456: 337-346, 2013.
27. Pan Y, Liu G, Zhou F, Su B and Li Y: DNA methylation profiles in cancer diagnosis and therapeutics. Clin Exp Med 18: 1-14, 2018.
28. Zhang HH, Hu J, Zhou YL, Qin X, Song ZY, Yang PP, Hu S, Jiang X and Xu GY: Promoted interaction of nuclear factor-kB with demethylated purinergic P2X3 receptor gene contributes to neuropathic pain in rats with diabetes. Diabetes 64: 4272-4284, 2015.
29. Zhou YL, Jiang GQ, Wei J, Zhang HH, Chen W, Zhu H, Hu S, Jiang X and Xu GY: Enhanced binding capability of nuclear factor-kB with demethylated P2X3 receptor gene contributes to cancer pain in rats. Pain 156: 1892-1905, 2015.
30. Choi HI, Ma SK, Bae EH, Lee JU and Kim SW: Peroxiredoxin 5 protects TGF-β induced fibrosis by inhibiting stat3 activation in rat kidney interstitial fibroblast cells. PLoS One 11: e0149266, 2016.
31. Chen T, You Y, Jiang H and Wang ZZ: Epithelial-mesenchymal transition (EMT): A biological process in the development, stem cell differentiation, and tumorigenesis. J Cell Physiol 232: 3261-3272, 2017.
32. Acloque H, Ocaña OH, Matheu A, Rizzoti K, Wise C, Lovell-Badge R and Nieto MA: Reciprocal repression between Sox3 and snail transcription factors defines embryonic territories at gastrulation. Dev Cell 21: 546-558, 2011.
33. Correa-Costa M, Andrade-Oliveira V, Braga TT, Castoldi A, Aguiar CF, Origassa CST, Rodas ACD, Hiyane MI, Malheiros DMAC, Rios FJO, *et al*: Activation of platelet-activating factor receptor exacerbates renal inflammation and promotes fibrosis. Lab Invest 94: 455-466, 2014.
34. Ruscetti M, Quach B, Dadashian EL, Mulholland DJ and Wu H: Tracking and functional characterization of epithelial-mesenchymal transition and mesenchymal tumor cells during prostate cancer metastasis. Cancer Res 75: 2749-2759, 2015.
35. Grande MT, Sanchez-Laorden B, Lopez-Blau C, De Frutos CA, Boutet A, Arévalo M, Rowe RG, Weiss SJ, López-Novoa JM and Nieto MA: Snail1-induced partial epithelial-to-mesenchymal transition drives renal fibrosis in mice and can be targeted to reverse established disease. Nat Med 21: 989-997, 2015.
36. Ahn HM, Yoo JW, Lee S, Lee HJ, Lee HS and Lee DS: Peroxiredoxin 5 promotes the epithelial-mesenchymal transition in colon cancer. Biochem Biophys Res Commun 487: 580-586, 2017.
37. Stewart D, Killeen E, Naquin R, Alam S and Alam J: Degradation of transcription factor Nrf2 via the ubiquitin-proteasome pathway and stabilization by cadmium. J Biol Chem 278: 2396-2402, 2003.
38. Nguyen T, Sherratt PJ, Huang HC, Yang CS and Pickett CB: Increased protein stability as a mechanism that enhances Nrf2-mediated transcriptional activation of the antioxidant response element. Degradation of Nrf2 by the 26 S proteasome. J Biol Chem 278: 4536-4541, 2003.